RANDOM WALKS AND PLANE ARRANGEMENTS IN THREE DIMENSIONS

LOUIS J. BILLERA, KENNETH S. BROWN, AND PERSI DIACONIS

1. INTRODUCTION

The geometry of hyperplane arrangements in Euclidean space is a rich subject, which touches geometry [14], combinatorics [21], and operations research [23]. Probability was introduced into the subject by Bidigare, Hanlon, and Rockmore [2], who found a natural family of random walks associated with hyperplane arrangements. These walks were studied further by Brown and Diaconis [6]. One reason this development is exciting is that the walks admit a rather complete theory. We introduce the reader to this circle of ideas by specializing to the 3-dimensional case (planes in $\mathbb{R}^3$). Here we are able to use tools from geometry to obtain a surprising formula for the stationary distribution of the walk.

1.1. **The geometric setup.** Consider a collection $\mathcal{A}$ of n planes through the origin in $\mathbb{R}^3$. We assume throughout this paper that the intersection of the planes is $\{0\}$. In particular, $n \geq 3$. It is useful to picture the arrangement $\mathcal{A}$ via the intersection of the planes with the unit sphere S^2. See Figure 1 for the case where $\mathcal{A}$ consists of the three coordinate planes. The picture shows the Northern Hemisphere, viewed
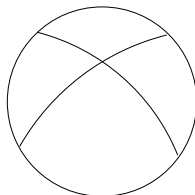

FIGURE 1. Three great circles on S^2.

from above the North Pole; thus the outer circle is the equator $z = 0$. Adding the plane $z = x + y$ gives the picture in Figure 2.
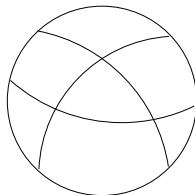

FIGURE 2. Four great circles on S^2.

The n great circles corresponding to the arrangement $\mathcal{A}$ decompose the sphere into cells: There are f_0 vertices, f_1 edges, and f_2 regions. When $n = 3$, for example, one has $f_0 = 6$, $f_1 = 12$, and $f_2 = 8$. Only the cells in the Northern Hemisphere are visible in the picture, but the Southern Hemisphere has exactly the same geometry. Notice that all the regions are triangular in Figure 1. In Figure 2 there are $f_2 = 14$ 2-dimensional cells: 8 triangles and 6 quadrilaterals, half of which are visible.

The cell decomposition induced by an arrangement has the following special property: *Given a region C and a vertex v, there is a unique region C' adjacent to v that is closest to C, in the sense that C' is separated from C by the minimum number of great circles.* The region C' is said to be the *projection* of C on v and is denoted vC. We explain in Section 3.2 why it is uniquely defined. Figure 3 shows an example; here C' is at distance two from C.
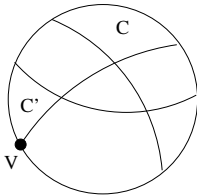

FIGURE 3. The projection of C on v.

1.2. **A random walk on the regions.** Bidigare, Hanlon, and Rockmore [2] used the projection operators to define the following walk on the regions: If the walk is in region C, choose a vertex v at random and move to the projection $C' = vC$. (We assume here that the vertices are chosen uniformly, so that all f_0 vertices are equally likely.) This walk is described mathematically by its *transition matrix K*. The rows and columns of K are indexed by the regions, with $K(C, C')$ being the chance of moving from C to C' in one step. Thus

$$K(C, C') = \frac{1}{f_0}\Lambda(C, C'),$$

where $\Lambda(C, C')$ is the number of vertices v of C' such that $vC = C'$.

Suppose, for instance, that $\mathcal{A}$ consists of the three coordinate planes. The 8 triangular regions are the intersections with the sphere of the 8 orthants in $\mathbb{R}^3$, as indicated in Figure 4. For example, the region $+-+$ corresponds to the orthant $x > 0$, $y < 0$, $z > 0$. The matrix Λ is shown in Table 1; one has $K = \frac{1}{6}\Lambda$.
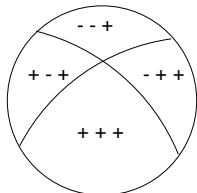

FIGURE 4. The regions correspond to orthants.

	+++	++−	+−+	+−−	−++	−+−	−−+	−−−
+++	3	1	1	0	1	0	0	0
++−	1	3	0	1	0	1	0	0
+−+	1	0	3	1	0	0	1	0
+−−	0	1	1	3	0	0	0	1
−++	1	0	0	0	3	1	1	0
−+−	0	1	0	0	1	3	0	1
−−+	0	0	1	0	1	0	3	1
−−−	0	0	0	1	0	1	1	3

TABLE 1. The matrix Λ.

Notice that for any region C, the three vertices of C satisfy $vC = C$; this explains the diagonal entries of Λ. Projection onto each of the remaining three vertices flips C to an adjacent region, thus accounting for the three 1's in each row. At each step, then, the walk stays in its current region with probability $1/2$ and otherwise moves to a randomly chosen adjacent region. This example is unusual, in that one never moves a distance of more than 1 in any step; typically the walk is much more vigorous.

The ℓth power of the matrix K gives the transition probabilities after ℓ steps; for example,

$$K^2(C, C') = \sum_{C''} K(C, C'') K(C'', C'),$$

which is the chance of moving from C to C' in two steps. After all, to get from C to C' in two steps the walk must go to some C'' and then to C'.

A fundamental theorem of Markov chain theory [17, Theorem 4.1.4] implies that $K^\ell(C, C')$ tends to a limit $\pi(C')$, independent of the starting region C:

$$K^\ell(C, C') \to \pi(C') \quad \text{as } \ell \to \infty.$$

(The theorem requires a mild regularity condition, which is satisfied by our chain.) Here π is a probability distribution on the set of regions, and $\pi(C')$ represents the chance that the random walk is in C' after a large number of steps from any starting region C. The distribution π is called the *stationary distribution* of the walk. It can be characterized as the unique probability distribution satisfying

$$\tag{1} \sum_{C} \pi(C) K(C, C') = \pi(C')$$

for all C'. This says that π, viewed as a row vector, is a left eigenvector for K with eigenvalue 1.

1.3. **Analysis of the walk.** Bidigare, Hanlon, and Rockmore [2] determined the eigenvalues of K, which turn out to be real (and even rational):

(a) 1 is an eigenvalue of multiplicity 1.
(b) For each plane $H \in \mathcal{A}$, there is an eigenvalue

$$\lambda_H = \frac{\# \text{ of vertices on } H \cap S^2}{f_0}$$

of multiplicity 1.
(c) $2/f_0$ is an eigenvalue of multiplicity $(f_2 - 2)/2$.

(d) 0 is an eigenvalue of multiplicity $(f_2 - 2)/2 - n + 1$.

A different proof of this can be found in [6], where it is shown further that K is diagonalizable. Yet another proof is given in [5]. For a simple example, take $n = 3$ again; the 8 eigenvalues are then $1, \frac{2}{3}, \frac{2}{3}, \frac{2}{3}, \frac{1}{3}, \frac{1}{3}, \frac{1}{3}, 0$.

A second result of [2, 6] is a surprisingly simple estimate relating the eigenvalues to the rate of convergence to stationarity. Let K_C^ℓ be the distribution of the walk started from C after ℓ steps, i.e., $K_C^\ell(C') = K^\ell(C, C')$. We measure convergence rate by means of the distance $\|K_C^\ell - \pi\|$ defined as follows: If P and Q are probability distributions on a finite set X, then

$$(2) \qquad \|P - Q\| = \max_{A \subseteq X} |P(A) - Q(A)|.$$

The version of the convergence rate estimate given in [6] is

$$(3) \qquad \|K_C^\ell - \pi\| \le \sum_{H \in \mathcal{A}} \lambda_H^\ell,$$

for any starting region C. When $n = 3$, for example, the distance to stationarity is bounded by $3\left(\frac{2}{3}\right)^\ell$ after ℓ steps.

Finally, a method is given in [6] for computing the stationary distribution π, though it is not always easy to get a useful formula for π by this method. Our main result is an explicit formula for π in the 3-dimensional case:

Theorem 1. *Let $\mathcal{A}$ be an arrangement of n planes in $\mathbb{R}^3$ whose intersection is $\{0\}$. Let π be the stationary distribution of the random walk on regions of the sphere, as described above. If C is a region with i sides, then*

$$\pi(C) = \frac{i - 2}{2(f_0 - 2)}.$$

We find this result quite surprising. It is not even obvious to us why all i-gons should have the same stationary probability, let alone why this probability should be proportional to $i - 2$. In our $n = 3$ example, the theorem says that the stationary distribution is uniform: $\pi(C) = \frac{1}{8}$ for each of the 8 triangles C.

1.4. **Organization of the paper.** In Section 2 we make several remarks about the main theorem and illustrate it with examples. In Section 3 we explain how to describe vertices, edges, and regions by means of sign sequences; this description is used in the proof of our main theorem. Section 4 gives some background on hyperplane arrangements in order to put the results stated in Section 1.3 into a broader context. We also state in Section 4 some of the results of [2, 6] that were specialized to the 3-dimensional case in 1.3. In Section 5 we show how the general theory specializes to card shuffling and random tiling models. We work out some 3-dimensional cases of this in detail. Sections 4 and 5 are included mainly for motivation; they are not needed for the proof of Theorem 1. The proof of the latter begins in Section 6, where we give a geometric description of the matrix K. With this description available, it is quite easy to complete the proof; we do this in Section 7. Finally, Section 8 contains some pointers to the literature on plane arrangements in $\mathbb{R}^3$.

The key arguments of this paper represent the combinatorial essence of a hyperplane arrangement as a collection of sequences of signs; see Section 3. This can be abstracted to the notion of an oriented matroid. The present project makes a nice introduction to these ideas.

2. Examples and remarks

2.1. **General position.** The n planes are said to be in *general position* if no three of the planes have a nonzero intersection or, equivalently, if only two great circles pass through each vertex on the sphere. Many of the examples in this paper are in fact in general position; but the simplicial arrangements to be discussed in Section 2.3 are never in general position unless $n = 3$, nor are the arrangements in Section 5 below.

It is easy to count cells in the general position case. One finds

$$f_0 = n(n-1), \quad f_1 = 2n(n-1), \quad \text{and} \quad f_2 = n(n-1) + 2.$$

In fact, there are $\binom{n}{2}$ pairs of great circles, each determining a pair of antipodal vertices, whence the first equation. For the second equation, note that each of the n great circles is cut into $2(n-1)$ arcs by the other $n-1$ great circles. [Alternatively, count the vertex-edge pairs in two different ways to get $2f_1 = 4f_0$, so that $f_1 = 2f_0$.] Finally, the third equation can be proved by a straightforward inductive argument, or it can be deduced from the first two via Euler's relation $f_0 - f_1 + f_2 = 2$.

The list of eigenvalues λ and multiplicities m_λ given in Section 1.3 becomes

λ	m_λ
1	1
$2/n$	n
$1/\binom{n}{2}$	$\binom{n}{2}$
0	$\binom{n}{2} - n + 1$

And the convergence rate estimate (3) is

$$\|K_C^\ell - \pi\| \le n \left(\frac{2}{n}\right)^\ell.$$

This shows that the distance to the stationary distribution is small after $\ell = 2$ steps if n is large. In Section 6.3, after we have a geometric description of the transition matrix K, we describe a family $\mathcal{A}_n$ of arrangements of n planes in general position such that $\|K_C - \pi\| \ge c > 0$ for all n. In this sense the walk is close to stationary after 2 steps, but not after 1 in general.

Another feature of the general position case is that if one wants to carry out the random walk algorithmically, it is quite easy to pick a random vertex: First pick a pair of great circles at random, so that all $\binom{n}{2}$ are equally likely; this defines a pair of antipodal points. Now choose one of these two points with probability $\frac{1}{2}$.

Finally, Theorem 1 gives the following formula for the stationary distribution in the general position case:

$$\pi(C) = \frac{i - 2}{2(n(n-1) - 2)}$$

if C is an i-gon.

Here are some specific examples:

Example 1. For $n = 3$, the arrangement is combinatorially equivalent to that of Figure 1. There are 8 triangular regions, and the stationary distribution is $\pi(C) = \frac{1}{8}$ for all C.

Example 2. For $n = 4$ planes in general position (Figure 2) there are 14 regions: 8 triangles with stationary probability $\pi(C) = \frac{1}{20}$ and 6 quadrilaterals with $\pi(C) = \frac{2}{20}$.

Example 3. With $n = 5$ planes in general position, the situation is as in Figure 5 up to isomorphism. There are 10 triangles with $\pi(C) = \frac{1}{36}$, 10 quadrilaterals with $\pi(C) = \frac{2}{36}$, and 2 pentagons with $\pi(C) = \frac{3}{36}$.
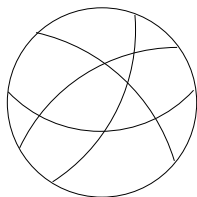

FIGURE 5. Five great circles in general position.

Example 4. With $n = 6$ or more planes the number of regions of each type can vary with the actual arrangement. From the catalogue in Grünbaum [12, 14] one sees that up to combinatorial equivalence there are exactly four general position arrangements of 6 planes, as shown in Figure 6. The number of i-gons ($i = 3, 4, 5, 6$)
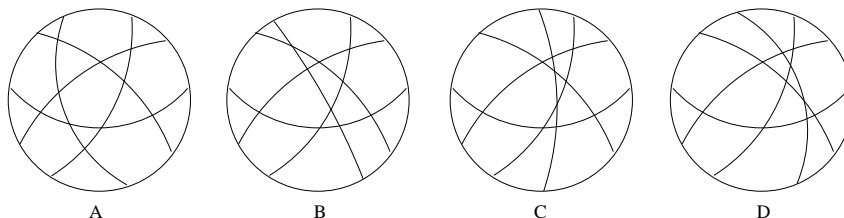

FIGURE 6. Six great circles in general position.

for each of these four arrangements is shown in Table 2. Each arrangement has $n(n-1) + 2 = 32$ regions. For each arrangement, the stationary probability of an i-gon is $\frac{i-2}{56}$. Note that, for some values of i, some arrangements don't have any i-gons. Nonetheless, the stationary probabilities sum to 1.

i	A	B	C	D
3	20	14	12	12
4	0	12	16	18
5	12	6	4	0
6	0	0	0	2

TABLE 2. The number of i-gons.

2.2. **The Euler relation.** For a given arrangement of n planes, let p_i be the number of i-sided regions. Since the stationary probabilities in Theorem 1 must sum to 1, we get

$$(4) \qquad \sum_{i=3}^{n} p_i \frac{(i-2)}{2(f_0 - 2)} = 1.$$

We now show that this relation is equivalent to the Euler relation $f_0 - f_1 + f_2 = 2$. Rewrite (4) as $\sum i p_i - 2 \sum p_i = 2(f_0 - 2)$. The first sum is the number of pairs consisting of a region and an edge of that region; since each edge is on exactly two regions, this sum equals $2f_1$. The second sum is f_2, so (4) becomes $2f_1 - 2f_2 = 2(f_0 - 2)$, which is Euler's identity.

2.3. **Simplicial arrangements.** The arrangement $\mathcal{A}$ is said to be *simplicial* if every region on the sphere is a triangle. The simplicial case has long held a special fascination for geometers [13, 14]. And it is of special interest for the probability story also. In fact, every arrangement has some triangles (at least n of them by Levi's theorem [14, p. 25]); so Theorem 1 has the following consequence:

Proposition 1. *The random walk on regions has a uniform stationary distribution if and only if the arrangement is simplicial.*

There are three known infinite families of simplicial arrangements and 90 "sporadic" examples. It has been conjectured that there are no more infinite families and at most finitely many additional sporadic examples; see [14, p. 8, Conjecture 2.1]. A catalogue showing the first 89 sporadic examples can be found in [13], and the 90th is in [14]. (Note: It is stated in [14] that there are 91 sporadic examples, but the arrangements called $A_2(17)$ and $A_7(17)$ in [13] have been shown to be isomorphic; see [15, p. 59].) Many of the examples have a great deal of symmetry, and one is therefore not surprised when the stationary distribution turns out to be uniform. But there is one known example ([14, pp. 8–9]) of a simplicial arrangement whose group of combinatorial symmetries is trivial. Nevertheless, the walk on the regions has a uniform stationary distribution. This example, which has $n = 28$, is shown in Figure 7 in its projective representation. We discuss such representations in Section 8; for now, suffice it to say that we get the spherical representation by drawing the lines in Figure 7 as great semicircles on the Northern Hemisphere. Parallel lines yield great semicircles with the same endpoints on the equator.

2.4. **Arrangements of pseudocircles.** The theory developed in [6] and in the present paper goes through if the family of great circles is replaced by a family of "pseudocircles", i.e., simple closed curves on the sphere that are not necessarily great circles but merely intersect as great circles would. See [4, 14, 23] for the precise definition and many examples. The reason the theory goes through is that, as we remarked in the introduction, all of our work is based on the oriented matroid underlying the arrangement, and this exists for arrangements of pseudocircles also. Generalizing in this way is of interest because it vastly increases the supply of examples. In particular, one obtains seven new infinite families of simplicial arrangements; see [14, 11].

3. An encoding of the cells

In Figure 4 we labeled each region on the sphere by a vector $(\sigma_1, \sigma_2, \sigma_3)$ of signs $+, -$. In this section we give a similar encoding of the regions, as well as the vertices
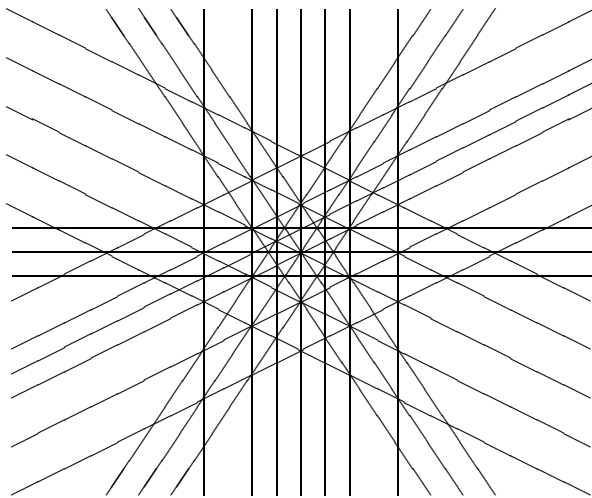
FIGURE 7. A simplicial arrangement with no symmetry (projective picture); the line at infinity is included.

and edges, for an arbitrary arrangement. This encoding is used in the proof of our main theorem in Section 7. The sign vectors are easier to think about if we replace each cell e by the cone over e, i.e., by the set of positive scalar multiples of e. We begin by establishing the language for talking about these cones.

3.1. **Chambers.** The open regions into which $\mathbb{R}^3$ is cut by $\mathcal{A}$ are called *chambers*. For example, if $\mathcal{A}$ consists of the three coordinate hyperplanes, the chambers are the 8 open orthants. The regions on the sphere that we have been discussing are simply the intersections of the chambers with the sphere.

We can describe a chamber by specifying, for each $H \in \mathcal{A}$, which side of H the chamber is on. To formalize this, write $\mathcal{A} = \{H_i\}_{i \in I}$ and let H_i^+ and H_i^- be the two open halfspaces determined by H_i. (The choice of which one to call H_i^+ is arbitrary but fixed.) Then the chambers are precisely the nonempty sets of the form

$$C = \bigcap_{i \in I} H_i^{\sigma_i},$$

where $\sigma_i = \pm$. The vector of signs $(\sigma_i)_{i \in I}$ provides a succinct description of C. Figure 8 illustrates this (using the spherical picture) for the four planes $x = 0$, $y = 0$, $z = 0$, $z - x - y = 0$. The region labeled $++++$, for instance, corresponds to the chamber $x > 0$, $y > 0$, $z > 0$, $z - x - y > 0$. Notice that the sign vectors of the remaining chambers can be filled in once $++++$ has been identified; just move from chamber to chamber, crossing one plane at a time and recording the appropriate sign change.

3.2. **Faces, products, and projections.** The chambers are defined by finitely many linear inequalities, so they are polyhedra. They have faces, which are the nonempty sets obtained by changing zero or more inequalities to equalities. For example, the chamber $++++$ in Figure 8 has a face defined by $x = 0$, $y > 0$, $z > 0$,
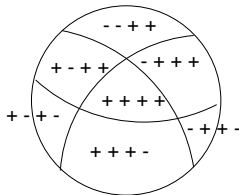
FIGURE 8. Sign vectors for four planes in general position.

$z - x - y > 0$. We say that this face has sign vector $0+++$. In general, the sign vector of a face F is the vector (σ_i) such that

$$F = \bigcap_{i \in I} H^{\sigma_i},$$

where $\sigma_i \in \{+, -, 0\}$ and $H_i^0 = H_i$. In Figure 8, the chamber $++++$ has three faces of codimension 1, with sign sequences $0+++$, $+0++$, and $+++0$. These correspond to the three sides of the triangle labeled $++++$ in Figure 8. Note that $++0+$ does not occur, because it would correspond to the inconsistent set of conditions $x > 0$, $y > 0$, $z = 0$, $z - x - y > 0$.

Let $\mathcal{C}$ be the set of chambers and let $\mathcal{F}$ be the set of faces of chambers; note that $\mathcal{C} \subset \mathcal{F}$ according to our conventions. Somewhat surprisingly, there is a naturally defined product on $\mathcal{F}$ that makes it a semigroup: Given $F, G \in \mathcal{F}$ with sign vectors $\sigma(F), \sigma(G)$, their product FG is the face with sign vector

$$\sigma_i(FG) = \begin{cases} \sigma_i(F) & \text{if } \sigma_i(F) \neq 0 \\ \sigma_i(G) & \text{if } \sigma_i(F) = 0. \end{cases}$$

This has a geometric interpretation: If we move on a straight line from a point of F toward a point of G, then FG is the face we are in after moving a small positive distance.

Given $F \in \mathcal{F}$ and $C \in \mathcal{C}$, their product FC is again a chamber, called the *projection* of C on F. It can be characterized as the nearest chamber to C having F as a face. Here "nearest" refers to the number of hyperplanes in $\mathcal{A}$ separating C from FC. This proves the existence of the projection operators that were used to construct the random walk in Section 1.

We continue to identify chambers and faces with their intersections with the sphere. Thus we have a cell decomposition of the sphere, with a semigroup structure on the set of cells. The next subsection illustrates the use of sign vectors and the semigroup structure.

3.3. **The diameter of the walk in $\mathbb{R}^3$.** Consider an arrangement in $\mathbb{R}^3$ and the walk on regions defined in Section 1. It is easy to see that there is an integer $\ell > 0$ such that $K^\ell(C, C') > 0$ for all C, C'; in other words, one can get from any region to any other in ℓ steps. The smallest such ℓ is called the *diameter* of the walk. As an example, consider the arrangement of three planes shown (in its spherical representation) in Figure 1. By inspection, to get from a chamber to its antipode by steps of the walk (through a choice of vertices) takes three steps, and this is in fact the diameter.

Proposition 2. *The diameter of the walk based on n planes in $\mathbb{R}^3$ is always either 2 or 3. It is 2 if $n \geq 5$ and the planes are in general position.*

Proof. One can never get from a region C to its antipode $-C$ in one step; in fact, each vertex v has at least two 0's in its sign vector, so multiplying by v cannot change all the signs of C. This shows that the diameter is at least two.

Consider two regions C, C', with C' an m-gon. Assume, to simplify notation, that the sign vector σ' of C' has $\sigma'_j = +$ for all j and that the first m components correspond to the m sides of C'. Then C' is the unique region whose sign vector has $+$ in its first m positions. If $m \geq 4$, we can find vertices v, w of C' such that v is on two of the sides of C' and w is on two different sides. Thus the sign vector of v has 0 in two of the first m slots and $+$ in the rest, and similarly for w, with the 0's of v and w in disjoint positions. The product vwC in the semigroup $\mathcal{F}$ therefore has $+$ in its first m positions, i.e., $vwC = C'$, and we can get from C to C' in two steps. This does not work if C' is a triangle ($m = 3$), but in that case we can get from any C to C' by using all three of the vertices of C'. Thus we have proved that the diameter is at most 3.

Finally, suppose that the planes are in general position, that $m = 3$, and that $n \geq 5$. Let w be a vertex on two of the great circles other than the three forming the sides of C'. In view of general position, the first 3 components of the sign vector of w are nonzero. Replacing w by $-w$ if necessary, we may assume that two of these 3 components, say the first two, are $+$. Let v be the vertex of C' whose sign vector has 0 in the first two slots. Then vw has $+$ everywhere, so we can get from C to C' in two steps. $\square$

4. Hyperplane arrangements

This section and the next are intended to provide some context for the seemingly strange random walk introduced in Section 1. We consider here arrangements of hyperplanes in spaces of arbitrary finite dimension d. The reader who wants to proceed to the proof of the main theorem may skip ahead to Section 6.

A good reference for the theory of hyperplane arrangements is the book by Orlik and Terao [20]. See also [19, 4, 23] and, for a concise summary of the basic concepts, [6, §2]. Throughout this section $\mathcal{A} = \{H_i\}_{i \in I}$ denotes a finite set of linear hyperplanes (subspaces of codimension 1) in a finite dimensional real vector space V. One often assumes that the intersection of the hyperplanes is the trivial subspace, as we have been assuming when $V = \mathbb{R}^3$. There is no loss of generality in making this assumption; for if it fails, then we can replace V by the quotient space V/V_0, where $V_0 = \bigcap_{i \in I} H_i$.

4.1. **Chambers, faces, and products.** The open regions into which V is cut by $\mathcal{A}$ are again called *chambers*. More precisely, the chambers are the connected components of the complement of $\bigcup_{i \in I} H_i$ in V. As in the 3-dimensional case, chambers and their faces are encoded by sign vectors $(\sigma_i)_{i \in I}$, where $\sigma_i \in \{+, -, 0\}$. The definition of the product of faces also remains unchanged, so we have a face semigroup $\mathcal{F}$ containing the set $\mathcal{C}$ of chambers, with $FC \in \mathcal{C}$ for $F \in \mathcal{F}$, $C \in \mathcal{C}$.

Remark. The faces are in 1–1 correspondence with their intersections with the unit sphere. If $\bigcap_{i \in I} H_i = \{0\}$, these intersections give a cell-decomposition of the sphere, as in the case $V = \mathbb{R}^3$.

4.2. **A walk on the chambers.** We may specify a random walk on $\mathcal{C}$ by assigning a weight w_F to each $F \in \mathcal{F}$. These weights satisfy $w_F \geq 0$ (many may be zero) and $\sum_{F \in \mathcal{F}} w_F = 1$. Given a starting chamber C_0, the walk proceeds by choosing from $\mathcal{F}$ with replacement, with w_F the chance of picking F each time. This generates choices $F_1, F_2, F_3, \ldots$. The walk proceeds by multiplying by F_i at stage i, i.e., by projecting onto F_i. Thus it goes

$$C_0, \ F_1 C_0, \ F_2 F_1 C_0, \ldots, F_i F_{i-1} \cdots F_1 C_0, \ldots.$$

The chance of moving from C to C' in one step is

$$(5) \qquad\qquad K(C, C') = \sum_{FC=C'} w_F.$$

The walk of Section 1 is based on n planes in $\mathbb{R}^3$ with $w_F = 0$ unless F is a half line (so that its intersection with the sphere is a point), and $w_F = 1/f_0$ for all half lines.

4.3. **Analysis of the walk.** As we remarked in the introduction, the hyperplane walks admit a rather complete theory. Bidigare, Hanlon, and Rockmore [2] give all the eigenvalues of the matrix K in a simple closed form. (We stated a special case of their result in Section 1.) Brown and Diaconis [6] prove diagonalizability of K and calculate eigenvalues using a chain complex given by the decomposition of the sphere by the hyperplanes. Brown [5] translates the walk to a semigroup setting and works out the appropriate Fourier analysis to get another proof of these results. The following result from [6] describes the stationary distribution and gives a bound on the convergence rate:

Theorem 2. *Let $\mathcal{A}$ be a hyperplane arrangement. Let $\{w_F\}$ be a probability distribution on the set $\mathcal{F}$ of faces. Let $K(C, C')$ be defined by* (5). *Then*

(a) *K has a unique stationary distribution π if and only if the weights $\{w_F\}$ are not concentrated on the faces in a single hyperplane, i.e., if and only if for each $H \in \mathcal{A}$ there is $F \nsubseteq H$ with $w_F > 0$.*
(b) *If the condition in (a) holds, then π may be described as follows: Sample* without *replacement from $\mathcal{F}$ according to the weights w_F. This generates an ordering $F_1, F_2, \ldots, F_m$ of $\{ F \in \mathcal{F} : w_F > 0 \}$. The product $F_1 F_2 \cdots F_m C_0$ is independent of C_0 and is a chamber distributed according to π.*
(c) *If the condition in (a) holds, then for any $C_0 \in \mathcal{C}$ and positive integer ℓ*

$$\|K_{C_0}^\ell - \pi\| \leq \sum_{H \in A} \lambda_H^\ell, \quad \text{where } \lambda_H = \sum_{F \subseteq H} w_F.$$

Part (c) of Theorem 2 immediately gives the convergence rate bound stated in Section 1. And part (b) of Theorem 2 can be used to get the explicit formula for π in the 3-dimensional case, as stated in Theorem 1. Indeed, we first discovered the formula by doing exactly that. It turns out, however, that one can give an easier and completely self-contained proof of Theorem 1 by a direct argument based on equation (1). That is what we do in Section 7.

5. Two examples

There are many hyperplane arrangements where the chambers can be labeled in a natural way by familiar combinatorial objects such as permutations or trees and the walk described in Section 4.2 captures a natural mixing process. In this section

we describe two such examples. The first is the braid arrangement, for which the chambers correspond to permutations. The action of faces on chambers gives natural shuffling schemes, such as the usual method of riffle shuffling a deck of cards, or a list rearrangement scheme used in computer science where a card is removed and replaced on top. The second example shows how hyperplane arrangements are related to tilings. In particular, we describe in some detail a hyperplane arrangement in $\mathbb{R}^3$ whose chambers correspond to rhombic tilings of a 10-gon. See [2, 6] for further examples.

5.1. **The braid arrangement and card shuffling.** The *braid arrangement* in $\mathbb{R}^d$ consists of the $\binom{d}{2}$ hyperplanes $H_{ij} = \{(x_1, \ldots, x_d) : x_i = x_j\}$ $(i < j)$. The chambers are associated with a common ordering of the coordinates and so with one of the $d!$ permutations. When $d = 4$, for example, one of the 24 chambers is the region defined by $x_1 > x_4 > x_2 > x_3$, corresponding to the permutation 1423.

The hyperplanes H_{ij} intersect in the line $x_1 = \cdots = x_d$. The braid arrangement therefore gives rise to an arrangement in a $(d-1)$-dimensional space, as explained at the beginning of Section 4. When $d = 4$, the resulting arrangement of 6 planes in $\mathbb{R}^3$ may be pictured as in Figure 9. The great circle corresponding to H_{ij} is labeled *i-j*. (The equator is *not* one of the great circles of the arrangement.) Each chamber is labeled with the associated permutation.

FIGURE 9. The braid arrangement when $d = 4$.

The faces of a chamber C are obtained by changing to equalities some of the inequalities defining C. For example, the chamber $x_2 > x_3 > x_1 > x_4$ has a face given by $x_2 > x_3 > x_1 = x_4$, which is also a face of the chamber $x_2 > x_3 > x_4 > x_1$. This common face is represented by the edge between 2314 and 2341 in Figure 9. Similarly, the vertex labeled 2 in the figure corresponds to the face $x_2 > x_1 = x_3 = x_4$; it is a face of six chambers, corresponding to the six possible orderings of the indices 1,3,4.

It is useful to encode the system of equalities and inequalities defining a face F by an ordered partition $(B_1, \ldots, B_k)$ of $\{1, \ldots, d\}$. Here $B_1, \ldots, B_k$ are disjoint nonempty sets whose union is $\{1, \ldots, d\}$; they are called the *blocks* of the partition,

and their order counts. For example, the face $x_2 > x_3 > x_1 = x_4$ corresponds to the 3-block ordered partition $(\{2\}, \{3\}, \{1, 4\})$, and the face $x_2 > x_1 = x_3 = x_4$ [vertex 2 in Figure 9] corresponds to the 2-block ordered partition $(\{2\}, \{1, 3, 4\})$. Notice that there is also a (unique) 1-block ordered partition, corresponding to the face $x_1 = x_2 = x_3 = x_4$. When we pass from $\mathbb{R}^4$ to a 3-dimensional quotient to make the hyperplanes have trivial intersection, this face becomes $\{0\}$. It does not show up in Figure 9 because its intersection with the sphere is empty.

The action of faces on chambers is easily pictured by thinking of a permutation $\tau = (\tau_1, \ldots, \tau_d)$ as the set of labels on a deck of d cards, with the card labeled τ_1 on top, and so on. The ordered partition $B = (B_1, B_2, \ldots)$ operates on τ by removing cards with labels in B_1 and placing them on top (keeping them in the same relative order), then removing cards with labels in B_2 and placing them next, and so on. Suppose, for example, that $d = 10$, $\tau = (1, 7, 3, 9, 10, 4, 5, 2, 6, 8)$, and $B = (\{2, 5\}, \{3, 4, 6, 10\}, \{7\}, \{1, 8, 9\})$; then B acting on τ gives $(5, 2, 3, 10, 4, 6, 7, 1, 9, 8)$.

The walk on chambers described in Section 4 now yields a variety of shuffling schemes, depending on the choice of weights w_F. One example that has received much attention is the "Tsetlin library", or "random-to-top" shuffle. Here one assigns a positive weight w_i to each 2-block ordered partition $(\{i\}, \{1, \ldots, d\} \setminus \{i\})$, and weight 0 to the other faces. When $d = 4$, for example, the vertices with positive weight are those labeled 1,2,3 in Figure 9 and the one that would be labeled 4 if it were visible. [The opposite vertex is shown as an open circle.] In the resulting random walk, a card is repeatedly picked at random according to the weights w_i and is replaced on top. This walk is useful in connection with self-organizing list-management schemes [9]. Imagine, for instance, a stack of d files, where file i is used with frequency w_i. Each time a file is used, it is replaced on top of the stack. After the process has been running for a long time, the most frequently used files will tend to be near the top.

The basic walk studied in this paper, where the vertices are weighted uniformly, is itself quite interesting when applied to the braid arrangement. Here, we assign weight $1/(2^d - 2)$ to each of the $2^d - 2$ two-block ordered partitions. The corresponding shuffling mechanism consists of "inverse riffle shuffles". In an ordinary riffle shuffle a deck of cards is divided into two piles, which are riffled together. The inverse chooses a set S of cards, which are removed ("unriffled") and placed on top; the $2^d - 2$ proper nonempty subsets S are all equally likely to be unriffled. This is very closely related to a standard model for riffle shuffling. See [2, 6] for further details and references to earlier work.

To conclude, let us apply the results of Section 1.3 to the walk when $d = 4$ and the vertices are chosen uniformly. There are 14 vertices, 36 edges, and 24 regions. The stationary distribution is uniform because each of the regions has three sides. The eigenvalues and multiplicities (λ, m_λ) are $(1, 1)$, $(\frac{3}{7}, 6)$, $(\frac{1}{7}, 11)$, and $(0, 6)$. After shuffling ℓ times, the distance to stationarity satisfies

$$\|K^\ell - \pi\| \le 6 \left(\frac{3}{7}\right)^\ell.$$

This bound shows that $\ell = 5$ shuffles suffice to make the distance to stationarity smaller than $1/10$.

5.2. **Arrangements and tilings.** We discuss now an example of an arrangement in $\mathbb{R}^3$ in which the chambers correspond to certain tilings of a centrally symmetric

10-gon. The walks described in this paper can then be used to generate random tilings. Such tilings are of interest to physicists who study quasicrystals; see [8, 16] and the references cited there. This is an example of a very general theory whereby hyperplane arrangements can be associated with a set of tilings of special convex polytopes called zonotopes [3, §4]. A good introductory reference for the material in this subsection is [23, Lecture 7].

Given n pairwise linearly independent vectors $v_1, \ldots, v_n \in \mathbb{R}^d$, we define a convex polytope known as a *zonotope* by

$$Z(v_1, \ldots, v_n) := \left\{ \sum_i \lambda_i v_i \mid 0 \leq \lambda_i \leq 1 \right\}.$$

We call the v_i the *zones* of $Z(v_1, \ldots, v_n)$. When $d = 2$, $Z(v_1, \ldots, v_n)$ is a centrally symmetric $2n$-gon; this is illustrated in Figure 10 for the case $d = 2$ and $n = 5$, where the resulting zonotope is a 10-gon.
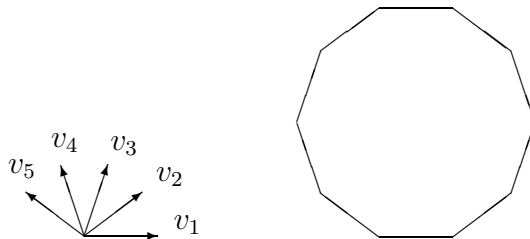
FIGURE 10. Five vectors in $\mathbb{R}^2$ and the 10-gon they generate.

We are interested in tilings of this 10-gon by the parallelograms generated by the $\binom{5}{2} = 10$ pairs v_i, v_j, $1 \leq i < j \leq 5$. Since we may take all the v_i to have the same length without loss of generality, we call these tilings *rhombic* tilings. Two such rhombic tilings are illustrated in Figure 11. It is a consequence of the work of
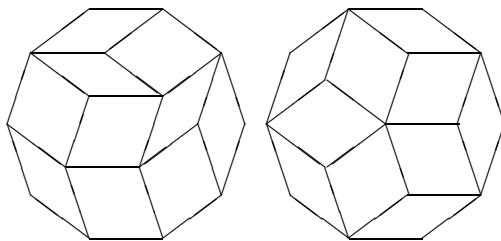

FIGURE 11. Two tilings of the 10-gon by parallelograms.

Billera and Sturmfels [3] that the set of all such tilings of this 10-gon corresponds to the chambers of an arrangement of $\binom{5}{3} = 10$ hyperplanes in $\mathbb{R}^3$. We describe this arrangement in some detail now.

Every triple v_i, v_j, v_k of the 5 given vectors, $1 \leq i < j < k \leq 5$, satisfies a unique (up to nonzero scalar) linear dependence relation. We write it as a relation among v_1, v_2, v_3, v_4, v_5, so it is given by a vector of length 5. Let $\tau = \{i, j, k\}$ and let the dependence be given by $z^\tau \in \mathbb{R}^5$; thus $\sum_{\ell=1}^5 z_\ell^\tau v_\ell = 0$ and $z_\ell^\tau = 0$ if $\ell \notin \tau$. The

span V of the z^τ, over all triples $\tau \subset \{1, 2, 3, 4, 5\}$, is the nullspace of the rank 2 matrix

$$A = \begin{pmatrix} x_1 & x_2 & x_3 & x_4 & x_5 \\ y_1 & y_2 & y_3 & y_4 & y_5 \end{pmatrix},$$

where $v_i = (x_i, y_i)$, and so is 3-dimensional. For each triple τ, we denote by $H^\tau \subset \mathbb{R}^5$ the hyperplane having z^τ as its normal (i.e., $H^\tau = \{x \in \mathbb{R}^5 \mid \langle x, z^\tau \rangle = 0\}$). The hyperplanes $\{H^\tau\}$ have a 2-dimensional intersection $V^\perp$ (the row space of A). We therefore get an arrangement in the 3-dimensional space $\mathbb{R}^5/V^\perp$ (which we may identify with V), as explained at the beginning of Section 4. This may be pictured as in Figure 12. Each great circle is labeled by the corresponding triple τ. Note
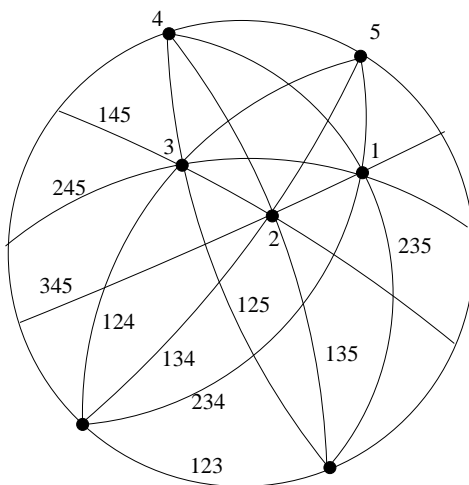

FIGURE 12. The arrangement associated to tilings of a 10-gon.

that the 4 great circles corresponding to triples $\tau \subset \{2, 3, 4, 5\}$ intersect at a pair of antipodal vertices, one of which is labeled 1 in Figure 12. This can be explained by straightforward linear algebra, which we leave to the interested reader. [Hint: Consider the matrix obtained from A by deleting the first column.] The other multiple intersections (with labels $2, \ldots, 5$) can be explained in a similar way.

We claim that the chambers of this arrangement correspond to the rhombic tilings of the 10-gon. To understand why this might be so, take any point $\theta = (\theta_1, \ldots, \theta_5) \in \mathbb{R}^5$ not on any of the hyperplanes H^τ. Lift the zones v_i to $\widetilde{v}_i = (x_i, y_i, \theta_i)$, $i = 1, \ldots, 5$, and form the 3-dimensional zonotope $\widetilde{Z} := Z(\widetilde{v}_1, \ldots, \widetilde{v}_5) \subset \mathbb{R}^3$. One can show that each 2-dimensional face of $\widetilde{Z}$ is a parallelogram. [Brief explanation: One first observes that the 2-dimensional faces of a 3-dimensional zonotope are translates of planar zonotopes spanned by subsets of the generating zones; see [23, p. 205]. These are all parallelograms unless three of the lifted zones $\widetilde{v}_i, \widetilde{v}_j, \widetilde{v}_k$ are linearly dependent. A linear dependence relation among these lifts would be a multiple of z^τ, where $\tau = \{i, j, k\}$. This would imply $\theta \in H^\tau$, contradicting the choice of θ.] Projecting the faces on the bottom of $\widetilde{Z}$ (i.e., the faces whose outer normal has a negative third coordinate) onto the 10-gon $Z(v_1, \ldots, v_5)$, one gets a rhombic tiling of the 10-gon. Further argument shows that any other θ

in the same chamber gives the same tiling and that all rhombic tilings of the 10-gon arise in this way.

An example of what might happen if the original zonotope were a hexagon and the lifted zonotope a 3-cube is shown in Figure 13; depending on its orientation in $\mathbb{R}^3$, the bottom of the cube would look like one of two tilings shown.
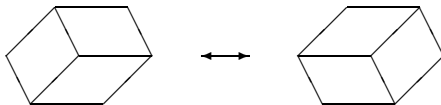

FIGURE 13. A flip of a 3-cube.

A move between adjacent chambers in the arrangement in Figure 12 corresponds to a simple local change in the corresponding tiling: for some embedded "3-cube" in the tiling, flip just that portion of the tiling as shown in Figure 13. So the chamber corresponding to a tiling is an i-gon if and only if the tiling has i embedded 3-cubes; for example the tiling on the left in Figure 11 corresponds to a triangular region, while that on the right corresponds to a pentagonal region.

We note that the situation described here is a piece of a very general theory of subdivisions [3, 1]. In particular, given a d-dimensional zonotope Z with n zones in $\mathbb{R}^d$, one can associate with it an arrangement of at most $\binom{n}{d+1}$ hyperplanes in $\mathbb{R}^{n-d}$ whose chambers correspond to certain tilings of Z. In our example it turns out to be *all* the rhombic tilings, but, in general, not all tilings can be obtained by the lifting procedure described in the example; see [3] for details. When $n = d + 3$ the derived arrangement is 3-dimensional, and so theory of the present paper applies.

To conclude, let us apply the results of Section 1.3 to our walk on the tilings of a 10-gon. There are 40 vertices, 100 edges, and 62 regions, with $(p_3, p_4, p_5) = (50, 10, 2)$. The stationary probability of a tiling with i cubes is $(i - 2)/76$. The eigenvalues and multiplicities (λ, m_λ) are $(1, 1)$, $(\frac{1}{4}, 10)$, $(\frac{1}{20}, 30)$, and $(0, 21)$. After ℓ steps, the distance to stationarity satisfies

$$\|K^\ell - \pi\| \le 10 \left(\frac{1}{4}\right)^\ell.$$

6. A geometric description of K

We return to the setting of Section 1, where $\mathcal{A}$ is a collection of planes in $\mathbb{R}^3$ with trivial intersection, and K is the transition matrix of the walk on the regions of the sphere (or, equivalently, on the chambers in $\mathbb{R}^3$). Recall that, in the notation of Section 1,

$$(6) \qquad K(C, C') = \frac{1}{f_0} \Lambda(C, C'),$$

where $\Lambda(C, C')$ is the number of vertices v of C' such that $vC = C'$. Note that $\Lambda(C, C)$ is the number of vertices of C and that $\Lambda(C, -C) = 0$. The main result of this section is the following formula for $\Lambda(C, C')$ when $C' \ne \pm C$: If k is the number of sides of C' for which the sign vectors of C and C' agree (that is, the number of planes in the arrangement that do *not* separate C from C'), then

$$\Lambda(C, C') = k - 1.$$

We prove this in Section 6.2 (Lemma 2). We begin by describing the matrix Λ in terms of lunes.

6.1. **Lunes.** For a region D and a vertex v of D, let $\ell(v, D)$ be the *lune* determined by v and D as in Figure 14. Thus if H_1 and H_2 are the great circles bounding D and passing through v, and if H_i^+ is the hemisphere defined by H_i that contains D ($i = 1, 2$), then $\ell(v, D)$ is the intersection $H_1^+ \cap H_2^+$. Given two regions C, C', we define the *lunacy* of C with respect to C' to be the number of vertices v of C' such that $C \subseteq \ell(v, C')$.
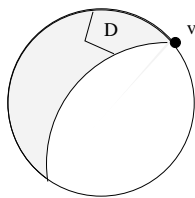

FIGURE 14. The lune $\ell(v, D)$

Proposition 3. *For any two regions C, C', $\Lambda(C, C')$ is equal to the lunacy of C with respect to C'.*

Proof. Assume, to simplify notation, that the sign vector of C' consists of all $+$'s. For a vertex v of C', we have $vC = C'$ if and only if the sign vector of vC is $+$ in the positions corresponding to the sides of C'. Now v has $+$ in all of these positions except two, where it has 0; so $vC = C'$ if and only if C already has $+$ in the two positions corresponding to the sides of C' that intersect at v. But this says precisely that $C \subseteq \ell(v, C')$. $\square$

Understanding K, then, reduces to calculating lunacy. Figure 15 shows a simple example; here C is in the lune $\ell(v, C')$ but not the other two C'-lunes, so $\Lambda(C, C') = 1$. On the other hand, C' is in two of the four C-lunes, so $\Lambda(C', C) = 2$. Note the lack of symmetry.
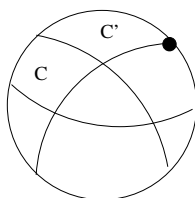

FIGURE 15. $\Lambda(C, C') = 1$.

There is a similar description of the transition matrix for the higher-dimensional hyperplane walks described in Section 4. One replaces the lunes by sets $\ell(F, C)$, where C is a chamber, F is a face of C, and $\ell(F, C)$ is an intersection of open half-spaces, one for each bounding hyperplane of C. What's special about the 3-dimensional case, however, is that lunacy is easy to compute. The computation depends on a simple geometric fact about polygons, related to "shellability".

6.2. **Shellability and the calculation of lunacy.** Consider a planar convex polygon P whose sides are extended to form lines $\ell_1, \ldots, \ell_n$. If the polygon is viewed from any point x outside of it, one sees a contiguous set of its edges, and these are precisely the edges whose lines separate x from P. See Figure 16; here it is assumed that P is on the positive side of each ℓ_i, and the lines are labeled with $\pm$ to indicate which side x is on.
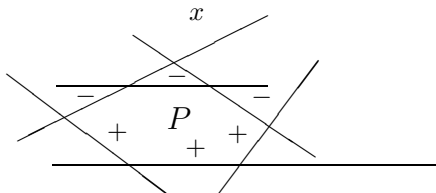

FIGURE 16. The sides visible from x.

All of this works equally well on the sphere:

Lemma 1 (Shelling lemma). *Given a spherical polygon bounded, in cyclic order, by n great circles $\ell_1, \ldots, \ell_n$, suppose that the interior of the polygon is on the positive side of each of these circles. Then any point on the sphere not on any of the circles is on the positive side of a cyclically contiguous subset of them.*

An analogue of the shelling lemma holds for convex polytopes in d-dimensional space [7] and for oriented matroids [18]. In the former case, contiguity is replaced by "shellability" of the set of visible faces, whence the name "shelling lemma". The latter case implies that everything we have done works for arrangements of pseudocircles (Section 2.4). See [23] and [4] for discussions of all of these topics. We omit a proof of the shelling lemma because it is treated thoroughly in the references cited and because, in the present low-dimensional case, it is quite believable from the picture.

Lemma 2 (Lunacy lemma). *Given two regions C and C' that are neither equal nor opposite, we have*

$$\Lambda(C, C') = k - 1,$$

where k is the number of sides of C' for which the sign vectors of C and C' agree. Consequently,

$$\Lambda(C, C') + \Lambda(-C, C') = i - 2$$

if C' is an i-gon.

In Figure 15, for example, C' has 3 sides, one of which separates C from C'; so $k = 2$ and $\Lambda(C, C') = 1$, as we have already observed.

Proof of the lunacy lemma. Assume that C' has sign vector $++\cdots+$ and apply the shelling lemma to the polygon C', with x equal to any interior point of C. It follows that the sign pattern of C, restricted to the sides of C', is a cyclic permutation of the string $++\cdots+--\cdots-$, where there are k +'s. Every pair of cyclically consecutive +'s corresponds to a lune of C' that contains C. Since there are $k - 1$ such pairs, the lunacy $\Lambda(C, C')$ is indeed $k - 1$. To prove the second assertion of the lemma, note that for each of the i sides of C' either C or $-C$ has the same sign as C'. Thus the k's for C and $-C$ sum to i. □

Remark. If $C = C'$, then $\Lambda(C, C') = i$, while if $C = -C'$ then $\Lambda(C, C') = 0$. Hence $\Lambda(C, C') + \Lambda(-C, C') = i$ rather than $i - 2$ if $C = \pm C'$.

6.3. **Convergence rate examples.** Recall from Section 2.1 that the walk on regions is close to stationary after 2 steps for an arrangement of n planes in general position if n is large. Now that we understand the matrix K, we can give an example where the walk is not close to stationary after 1 step, as advertized in Section 2.1. In other words, we want $\|K_C - \pi\|$ to be bounded away from 0 for an infinite family of general position arrangements with larger and larger n. We use a family of arrangements $\mathcal{A}_n$ constructed by Füredi–Palásti [10], for which p_3, the number of triangles, is asymptotic to $2n^2/3$ as $n \to \infty$. (Recall from Section 2.1 that f_2, the total number of regions, is about n^2. So there are about $n^2/3$ non-triangular regions. Most of these are hexagons.) Fix a starting region C. We claim that for any triangular region C', either $\Lambda(C, C') = 0$ or $\Lambda(C, -C') = 0$. To see this, we may assume $C' \neq \pm C$. Then $\Lambda(C, C') + \Lambda(-C, C') = 1$ by the lunacy lemma, so one term is 0. Our claim now follows from the fact that $\Lambda(-C, C') = \Lambda(C, -C')$.

In view of the claim, there are $p_3/2$ triangular regions C' that cannot be reached from C in one step. Our main theorem, however, implies that this set $\mathcal{T}$ of triangles has stationary probability

$$\pi(\mathcal{T}) = \frac{p_3}{2} \cdot \frac{1}{2(f_0 - 2)}.$$

The definition (2) of the distance between probability distributions now implies that $\|K_C - \pi\| \geq \pi(\mathcal{T})$, which tends to $1/6$ as $n \to \infty$. Thus the walk for $\mathcal{A}_n$ is not close to stationary after one step.

Remark. On the other hand, there is a naturally occurring family of arrangements $\mathcal{B}_n$ for which the walk *is* close to random after one step. Here $\mathcal{B}_n$ is the *cyclic* arrangement, consisting of n great circles that form the sides of an n-gon in the Northern Hemisphere. There is, of course, also an n-gon antipodal to this one in the Southern Hemisphere. $\mathcal{B}_n$ is a general position arrangement; for $n \geq 5$ there are $2n$ triangles and $n(n - 3)$ quadrilaterals in addition to the two n-gons. The cases $n = 3, 4, 5, 6$ are shown in Figures 1, 2, 5, and 6. A straightforward but tedious calculation shows that, for any starting region C, $\|K_C - \pi\| \leq c/n$ for c a universal constant; thus the walk for this family *is* close to random after one step when n is large.

7. Proof of Theorem 1

We are trying to calculate the stationary distribution of the walk with transition matrix given by (6). The assertion is that

$$(7) \qquad \pi(C) = \frac{i - 2}{2(f_0 - 2)}$$

if C is an i-gon. There are two ways to proceed.

Method 1. As we remarked in the introduction, it suffices to show that the right-hand side of (7) is a probability distribution satisfying

$$(8) \qquad \sum_C \pi(C) K(C, C') = \pi(C')$$

for all C'. Now we already know, by the Euler relation, that the right-hand side sums to 1 (Section 2.2). So it suffices to show, for each C', that

$$\sum_C (i(C) - 2)K(C, C') = i(C') - 2,$$

where $i(C)$ is the number of sides of C. Equivalently, we must show

(9) $$\sum_C (i(C) - 2)\Lambda(C, C') = f_0(i(C') - 2).$$

Since $i(-C) = i(C)$, we can replace $\Lambda(C, C')$ on the left by the average

$$M(C, C') = \frac{\Lambda(C, C') + \Lambda(-C, C')}{2}$$

without changing the value of the sum. In view of the lunacy lemma, the left side of (9) becomes

$$\sum_C (i(C) - 2)M(C, C') = \sum_C (i(C) - 2)\frac{i(C') - 2}{2} + 2(i(C') - 2),$$

where the second term takes account of the fact that $M(\pm C', C') = i(C')/2$ instead of $(i(C') - 2)/2$. Pulling out the factor $i(C') - 2$, and recalling that $\sum_C (i(C) - 2) = 2(f_0 - 2)$, we obtain (9). $\qquad\square$

Method 2. We know that π exists and is characterized by (8), which can be rewritten

(10) $$\sum_C \pi(C)\Lambda(C, C') = f_0\pi(C').$$

Since $\Lambda(C, C') = \Lambda(-C, -C')$, it follows that $\pi(-C) = \pi(C)$. We may therefore rewrite (10) as

$$\sum_C \pi(C)M(C, C') = f_0\pi(C'),$$

with M as in the first proof. Using the lunacy lemma (and taking account of the terms in the sum where $C = \pm C'$), the equation becomes

$$\sum_C \pi(C)\frac{i(C') - 2}{2} + 2\pi(C') = f_0\pi(C')$$

or, since $\sum_C \pi(C) = 1$,

$$\frac{i(C') - 2}{2} + 2\pi(C') = f_0\pi(C').$$

Solving for $\pi(C')$, we obtain

$$\pi(C') = \frac{i(C') - 2}{2(f_0 - 2)},$$

as required. $\qquad\square$

This second proof is somewhat more satisfying than the first, since equation (7) appears naturally, rather than being pulled out of a hat. Note also that the second proof did not use the Euler relation; it therefore has the Euler relation as a consequence. Note, finally, that Method 2 proves uniqueness of π (though not existence) without appeal to the theory of Markov chains.

Remark. We are mystified by the factor $i - 2$ in Theorem 1. To help appreciate the mystery (and Theorem 1) let us consider a different random walk on the chambers of a hyperplane arrangement, called the *local walk*. Suppose the walk is currently in region C bounded by i hyperplanes. Pick one of the bounding planes uniformly at random. The walk moves to the chamber adjacent to C along the chosen hyperplane. Call the transition matrix of this walk $H(C, C')$. If $i(C)$ denotes the number of sides of C, then

$$H(C, C') = \begin{cases} 1/i(C) & \text{if } C' \text{ is adjacent to } C \\ 0 & \text{otherwise.} \end{cases}$$

For this walk, an i-sided chamber C has stationary probability proportional to $i = i(C)$; moreover, this walk is reversible: $i(C)H(C, C') = i(C')H(C', C)$. The more vigorous walk $K(C, C')$ that we have been studying is not reversible except in special cases. It is one of only a few families of nonreversible walks where the stationary distribution is known explicitly. For the braid arrangement of Section 5.1, the local walk corresponds to mixing a deck of cards by adjacent transpositions, whereas the walk of this paper corresponds to the (much faster) riffle shuffling. For tilings (Section 5.2), physicists currently use the local walk (cube flips) for simulating a random tiling; see [22]. The walk described here may offer vast speed-ups.

8. Final remarks

The plane arrangements $\mathcal{A}$ in $\mathbb{R}^3$ that we have been considering in this paper occur in the literature under the name *line arrangements*. In fact, a plane through the origin in $\mathbb{R}^3$ is the same as a line in the projective plane P^2, so we can think of $\mathcal{A}$ as an arrangement of lines in the plane. Recall that the points of P^2 are the lines through the origin in $\mathbb{R}^3$. Since a line through the origin in $\mathbb{R}^3$ corresponds to a pair of antipodal points on the sphere S^2, we get a 2-to-1 map $S^2 \to P^2$. The great circles in our spherical pictures are the inverse images of the lines in P^2 under this map. As a practical matter, if P^2 is viewed as the affine plane with an extra line at infinity, one goes from the projective picture to the spherical picture by drawing the projective picture on the Northern Hemisphere, the line at infinity becoming the equator.

For a simple example, consider the arrangement of four lines in P^2 consisting of the three lines shown in Figure 17 together with the line at infinity. The corresponding spherical picture is Figure 2. A more complicated example of a projective picture was given in Figure 7. The cell-decomposition of S^2 that we have been using in this paper is obtained by lifting an analogous cell-decomposition of P^2. Thus there is a pair of antipodal cells in S^2 for each cell in P^2.
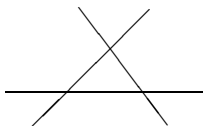

FIGURE 17. Four lines in P^2; the line at infinity is included.

There is an extensive literature on line arrangements (and "pseudoline" arrangements) going back to the 1820's. Much is known, but there are still many open

questions; see [14, 11] for surveys. Some of the more interesting results and open questions concern the polygon counts p_i ($i \geq 3$) where, following standard conventions, we now denote by p_i the number of i-gons in the cell decomposition of P^2; this is half of what was called p_i in Section 2. A sample result is that for an arrangement in general position, one has

$$(11) \qquad p_3 = 4 + \sum_{i \geq 5} (i - 4)p_i.$$

(The reader can check that this equation holds for each column of Table 2, after the numbers in that table are cut in half.) Moreover, given any sequence $p_3, p_5, p_6, p_7, \ldots$ of natural numbers satisfying (11), one can always find a general position arrangement with those polygon counts. One has no control over p_4, however, and, indeed, very little is known about p_4. Equivalently, one has no control over the number of lines in the arrangement. Thus we are still very far from knowing, for a given n, what vectors $(p_3, p_4, \ldots, p_n)$ can occur.

See [14, 11] for a wealth of further results, conjectures, and open questions.

Acknowledgments

References

1. Margaret M. Bayer and Keith A. Brandt, *Discriminantal arrangements, fiber polytopes and formality*, J. Algebraic Combin. **6** (1997), no. 3, 229–246.
2. T. Patrick Bidigare, Phil Hanlon, and Daniel N. Rockmore, *A combinatorial description of the spectrum for the Tsetlin library and its generalization to hyperplane arrangements*, Duke Math. J., to appear.
3. Louis J. Billera and Bernd Sturmfels, *Fiber polytopes*, Ann. of Math. (2) **135** (1992), no. 3, 527–549.
4. Anders Björner, Michel Las Vergnas, Bernd Sturmfels, Neil White, and Günter M. Ziegler, *Oriented matroids*, Encyclopedia of Mathematics and its Applications, vol. 46, Cambridge University Press, Cambridge, 1993.
5. Kenneth S. Brown, *Random walks and ring theory*, preprint, 1998.
6. Kenneth S. Brown and Persi Diaconis, *Random walks and hyperplane arrangements*, Ann. Probab., to appear.
7. H. Bruggesser and P. Mani, *Shellable decompositions of cells and spheres*, Math. Scand. **29** (1971), 197–205 (1972).
8. Veit Elser, *Random tiling structure of icosahedral quasicrystals*, Philosophical Magazine B **73** (1996), 641–656.
9. James Allen Fill, *An exact formula for the move-to-front rule for self-organizing lists*, J. Theoret. Probab. **9** (1996), no. 1, 113–160.
10. Z. Füredi and I. Palásti, *Arrangements of lines with a large number of triangles*, Proc. Amer. Math. Soc. **92** (1984), no. 4, 561–566.
11. Jacob E. Goodman, *Pseudoline arrangements*, Handbook of discrete and computational geometry (J. E. Goodman and J. O'Rourke, eds.), CRC Press, Boca Raton, 1997, pp. 83–109.
12. Branko Grünbaum, *Convex polytopes*, Pure and Applied Mathematics, vol. 16, Wiley-Interscience, New York, 1967, with the cooperation of Victor Klee, M. A. Perles and G. C. Shephard.
13. ———, *Arrangements of hyperplanes*, Proceedings of the Second Louisiana Conference on Combinatorics, Graph Theory and Computing (Louisiana State University, Baton Rouge, La., March 8–11, 1971) (R. C. Mullin, K. B. Reid, D. P. Roselle, and R. S. D. Thomas, eds.), Louisiana State University, 1971, pp. 41–106.
14. ———, *Arrangements and spreads*, CBMS Regional Conference Series in Mathematics, vol. 10, American Mathematical Society, Providence, R.I., 1972.

15. Branko Grünbaum and G. C. Shephard, *Simplicial arrangements in projective* 3*-space*, Mitt. Math. Sem. Giessen (1984), no. 166, 49–101.
16. Christopher L. Henley, *Random tiling models*, Quasicrystals: the state of the art (D. P. DiVincenzo and P. J. Steinhardt, eds.), Directions in Condensed Matter Physics, vol. 11, World Scientific Publishing Co. Inc., River Edge, NJ, 1991, pp. 429–524.
17. John G. Kemeny and J. Laurie Snell, *Finite Markov chains*, The University Series in Undergraduate Mathematics, D. Van Nostrand Co., Inc., Princeton, N.J.-Toronto-London-New York, 1960.
18. Arnaldo Mandel, *Topology of oriented matroids*, Ph.D. thesis, University of Waterloo, 1982.
19. Peter Orlik, *Introduction to arrangements*, CBMS Regional Conference Series in Mathematics, vol. 72, American Mathematical Society, Providence, R.I., 1989.
20. Peter Orlik and Hiroaki Terao, *Arrangements of hyperplanes*, Grundlehren der Mathematischen Wissenschaften, vol. 300, Springer-Verlag, Berlin, 1992.
21. Richard P. Stanley, *Enumerative combinatorics. Vol. 1*, Cambridge Studies in Advanced Mathematics, vol. 49, Cambridge University Press, Cambridge, 1997, with a foreword by Gian-Carlo Rota, corrected reprint of the 1986 original.
22. K. J. Strandburg, Lei-Han Tang, and M. V. Jaric, *Phason elasticity in entropic quasicrystals*, Physical Review Letters **63** (1989), 314–317.
23. Günter M. Ziegler, *Lectures on polytopes*, Graduate Texts in Mathematics, vol. 152, Springer-Verlag, New York, 1995.

Cornell University, Ithaca, NY 14853-7901
E-mail address: `billera@math.cornell.edu`

E-mail address: `kbrown@math.cornell.edu`